

# Analysis of one-dimensional photonic band gap structures with a liquid crystal defect towards development of fiber-optic tunable wavelength filters

**Ignacio Del Villar, Ignacio R. Matías and Francisco J. Arregui**

*Departamento Ingeniería Eléctrica y Electrónica, Universidad Pública de Navarra, 31006 Pamplona, Spain*  
[ignacio.delvillar@unavarra.es](mailto:ignacio.delvillar@unavarra.es), [natxo@unavarra.es](mailto:natxo@unavarra.es), [parregui@unavarra.es](mailto:parregui@unavarra.es)

**Richard O. Claus**

*Fiber & Electro-Optics Research Center, The Bradley Department of Electrical and Computer Engineering 106  
Plantation Road, Virginia Tech, Blacksburg, VA 24061, USA*

**Abstract:** A theoretical analysis of a fiber optical photonic band gap based tunable wavelength filter is presented. The design presented here is based on the quarter wave reflector with a liquid crystal defect layer in the middle of the structure. The filter generated by the structure is shifted in wavelength as the voltage applied to the structure is modified. Some critical parameters are analyzed: the effect of the consideration of fiber as the first layer and not the input medium in the shape of the filter, the number of layers of the structure, and the thickness of the defect layer. This last parameter determines the width of the wavelength sweep of the filter, but is limited by the creation of more defects. Some rules of practical implementation of this device are also given.

© 2003 Optical Society of America

**OCIS codes:** (050.2770) Gratings, (060.2340) Fiber optics components

---

## References and links

1. J. Tervo, M. Kuitinen, P. Vahimaa, J. Turunen, T. Aalto, P. Heimala, M. Leppilhalme, "Efficient Bragg waveguide-grating analysis by quasi-rigorous approach based on Redheffer's star product," *Opt. Comm.* **198**, 265 (2001).
2. P. Villeneuve, D. Abrams, S. Fan and J.D. Joannopoulos, "Single mode waveguide microcavity for fast optical switching," *Opt. Lett.* **21**, 2017 (1996).
3. P. Tran, "Optical switching with a nonlinear photonic crystal: a numerical study," *Opt. Lett.* **21**, 1138 (1996).
4. J. Broeng, D. Mogilevstev, S. E. Barkou and A. Bjarklev, "Photonic crystal Fibers: A New Class of Optical Waveguides," *Opt. Fiber Tech.* **5**, 305 (1999).
5. R. W. Ziolkowski and T. Liang, "Design and characterization of a grating-assisted coupler enhanced by a photonic-band-gap structure for effective wavelength-division demultiplexing," *Opt. Lett.* **22**, 1033 (1997).
6. T. D. James, A. C. Greenwald, E. A. Johnson, W. A. Stevenson, J. A. Wollam, T. George, and E. W. Jones, "Nano-Structured Surfaces For Tuned Infrared Emission For Spectroscopic Applications," *Proc. SPIE Opt. 2000. Photonics West, San Jose, CA, 22-28. January (2000)*.
7. J. D. Joannopoulos, R. D. Meade, and J. N. Winn, "Photonic crystals: Molding the Flow of Light," Princeton University Press (1995).
8. L. Sireto, G. Coppola, G. Abatte, G. C. Righini and J. M. Otón, "Electro-optical switch and continuously tunable filter based on a Bragg grating in a planar waveguide with liquid crystal overlayer," *Opt. Engineering* **41**, 2890 (2002).
9. E. Yablonovitch, "Photonic band-gap structures," *J. Opt. Soc. Am. A* **10**, 283 (1993).
10. F. J. Arregui, I. R. Matías, K. L. Cooper, R. O. Claus, "Fabrication of Microgratings on the Ends of Standard Optical Fibers by Electrostatic Self-Assembly Monolayer Process," *Opt. Lett.* **26**, 131 (2001).
11. F.J. Arregui, I.R. Matias, Y. Liu, K.M. Lenahan and R.O. Claus "Optical fiber nanometer-scale Fabry-Perot interferometer formed by the Ionic Self Assembly Monolayer Process," *Opt Lett.* **24**, 596 (1999).
12. F. J. Arregui, B. Dickerson, R. O. Claus, I. R. Matias, K. L. Cooper, "Polymeric thin films of controlled complex refractive index formed by the Electrostatic Self-Assembled Monolayer Process," *IEEE Phot. Tech. Lett.* **13**, 1319 (2001).

## 1. Introduction

Photonic crystals is a field with an enormous set of possible applications like waveguides [1], filters, switches [2,3], photonic crystal fiber [4], multiplexers [5] and sensors [6]. The reflection output obtained in the photonic band gaps originated by these structures is nearly complete, and the introduction of a defect permits that defect states, corresponding to localized modes in the defect, exist in the range of frequencies of the band gap [7]. The refractive index and the thickness of the defect define the position of the defect state in the photonic band gap. This property will be exploited in this paper for the design of a fiber-optic tunable wavelength filter formed by a photonic band gap (PBG) structure with periodicity in one dimension, which includes a defect layer with a refractive index that owns a dependence on a parameter.

Liquid crystals are materials that present a variation in their effective refractive index if an electric field is applied. In addition to this they are cost effective and easy to manipulate [8]; that is the reason for selecting this material instead of others dependent on the temperature or a mechanical force for instance. By changing the voltage applied to the structure, the defect state that constitutes the filter will sweep a range of wavelengths. However, it must be avoided that more than one defect state is created inside the band gap [9]. This fact depends on both the refractive index and the thickness of the defect [7]. Since the first one is the parameter that does not vary so much in comparison with its absolute value, the focus will be centered in thickness in terms of design. Other important applications of liquid crystals in the middle of one-dimensional PBG structures are electro-optical switches and modulators [8].

## 2. Structure of the tunable wavelength filter

The structure of the wavelength filter is represented in Fig. 1. There are two fibers placed end to end and aligned with the help of a precision positioner. The fibers should be single mode, so as to avoid the creation of a set of wave vectors. On each end of both fibers there is a deposition of a stack of alternatively high and low refractive index layers, and they are joined by a defect layer of smectic A\* liquid crystal, as suggested in Ref. [8]. This PBG structure is one dimensional, so it could be also understood in terms of distributed Bragg reflectors, but the sense for selecting PBG notation is the possibility of translating the idea towards 2D or 3D-PBGs because rules of design are roughly the same.

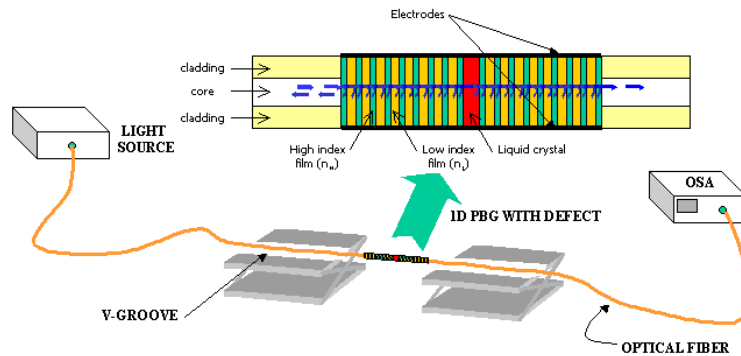


Fig. 1. Structure of the 1D PBG wavelength filter consisting of 2 Bragg mirrors of 30 layers and a cavity (defect)

The creation of a band gap is assured no matter which contrast between high and low refractive index layers there is, but this is deeper if the contrast is bigger. Another way of

increasing the depth is adding more layers to the structure. This effect leads also to the creation of thinner and sharper filters. The output signal will be detected in the Optical Spectrum Analyzer (OSA) at the other side of the fiber, showing the filtered signal of the light source. The sense of placing the defect in the middle is that the structures at each side constitute mirrors that bounce back and forth the light of one evanescent mode leading to the creation of a localized mode in the defect. With regard to the deposition of layers onto the extreme of both optical fiber pigtails, we have developed some experiments successfully by using the Electrostatic Self-Assembly Method (ESAM) [10-12].

The example presented corresponds to the 1D-PBG structure of Fig. 2, which is exactly the quarter-wave reflector (QWR) with the presence of a defect [3]. It has 61 layers and it has been designed so that the main band gap is centered at the standard wavelength of 1550 nm. Taking as reference the ESAM [10], the two types of layers present apart from the defect layer have a refractive index of  $n_H=1.8$  (corresponding to  $[\text{Au:PDDA}^+/\text{PSS}^-]_n$  bilayers) [11], and  $n_L=1.424$  (corresponding to  $[\text{PDDA}^+/\text{Pss}^-]_n$  bilayers) [12]. The incident and output media are the own optical fiber, and the index of the defect liquid crystal layer will be 1.65, that corresponds with the  $\theta = 10^\circ$  state of the BDH764E liquid crystal [8]. The values of  $\theta$  are produced by applying different voltages to the structure between  $+V$ , which corresponds with  $10^\circ$  and  $-V$ , which corresponds with  $-10^\circ$ . The thickness of the defect is 2370 nm.

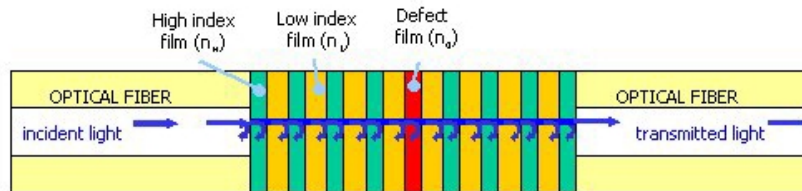


Fig. 2. 1D-PBG structure of 61 layers with a defect

The simulation of the transmission in this structure is obtained with a program developed based on the Rigorous Coupled Wave Analysis [13] for a total of 150000 points in the wavelength range between 400 and 2000 nm. The plot of Fig. 3 presents two band gaps centered at 1550 and 513 nm, corresponding with the first and third harmonics respectively, being the first wider. In both band gaps there is a defect state. If the thickness of the layers was changed maintaining the same period in the structure, the band gap of a second harmonic at 750 nm would be opened, but the depth of the other band gaps would be reduced. Consequently the topology of the structure proposed in Ref. [3] has been considered more adequate for showing the properties of defects in a deep band gap. Only if the input and output media have the same refractive index the unity transmission may be achieved, which is the case for this design.

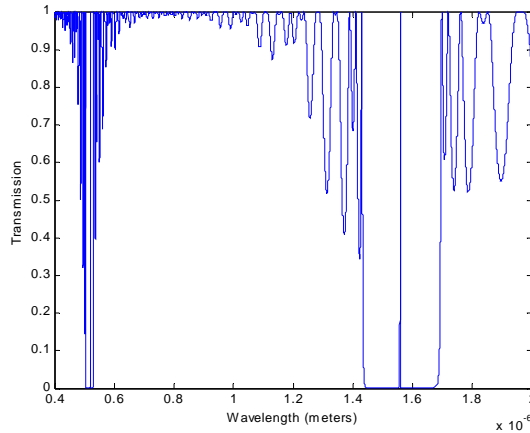


Fig. 3. Transmitted power of the quarter-wave reflector with the introduction of a defect in the middle

But if one includes the mismatch caused by an air-gap at the interface between the light source (or the OSA) and the optical fiber, slightly different results are obtained as shown in Fig. 4. For comparison, Fig. 4 also shows the calculated result when these air-gaps are ignored. The length of each fiber in this case is 1m. This plot is represented in logarithmic scale to show the similar influence of the fiber layers in the band gap and the rest of regions. The only remarkable difference is the presence of a ripple in the entire spectrum, caused by the two new Fabry Perot cavities of 1m length at both sides of the structure. This will not produce important changes in the results, but it will be considered in the rest of simulations.

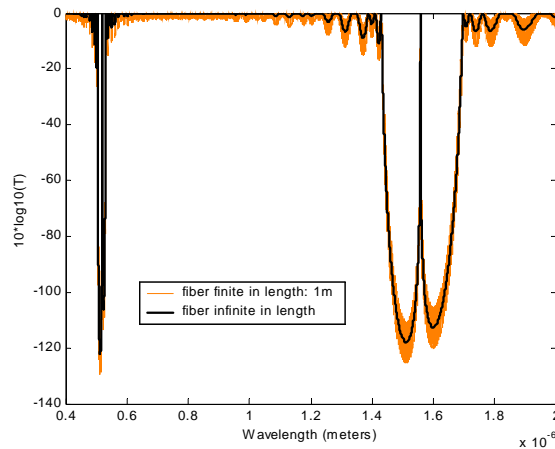


Fig. 4. Transmitted power of the quarter-wave reflector with the introduction of a defect in the middle considering both fibers infinite or finite in length

The amplitude of the ripple depends on the contrast of refractive indexes between the exterior media and the fiber, consequently it remains constant for any length of the fiber, whereas the frequency of the ripple is dependent on the length of the fiber. If the length of both fibers is different the lower will generate an envelope that will include the ripple generated by the bigger, but in the case studied here there is no envelope created because both fibers are equal in length. A way of avoiding the ripple is to have an exterior medium that is as close as possible to the refractive index of fiber, for instance an index matching gel.

### 3. Rules of design

Concerning the selection of 2370 nm of thickness for the defect, it is located beyond the limit that avoids the creation of more than one defect state inside the band gap. If the thickness of the defect is 2000 nm there are two defect states inside the band gap. However, as their position is shifted by the thickness of the defect, one of them leaves the band gap, and at 2370 nm there is only one defect state for the range of refractive indexes it is being studied. This is shown in Fig. 5 for three different thicknesses: 2170, 2270 and 2370 nm. For this figure and the next one the effect of considering the interfaces between output media and fibers is not considered because the ripple creates confusion for the reader.

Later on, for greater values than 2370 nm another state will enter the forbidden range of frequencies, and the effect is again that two defect states are present in the forbidden range of wavelengths. This effect is analyzed in Fig. 6, for two different thicknesses in the defect apart from the one studied in Fig. 3: 2450 and 2530 nm. If 10000 nm was selected five defect states would appear, and this number will increase as the thickness is greater. The same would happen for the variation of the refractive index, but it is quite low here: 0.02 nm. If another design is desired with an even wider sweep in wavelength, the thickness can be increased to higher values where more than one defect state is created. The drawback is that the band gap will be shared by the states present inside it and the window filtered will not be so wide.

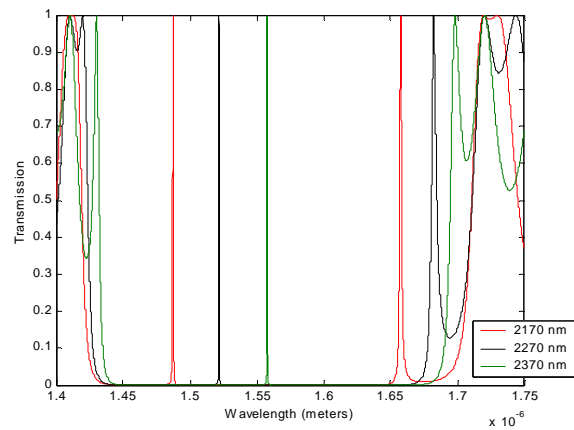


Fig. 5. Defect states in the band gap three different thicknesses of the liquid crystal layer. A defect state leaves the band gap.

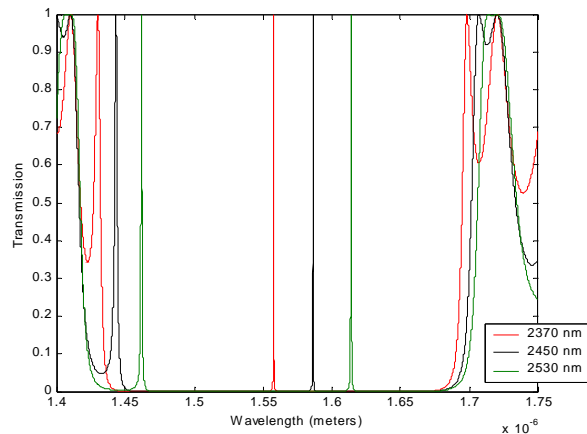


Fig. 6. Defect states in the band gap for three different thicknesses of the liquid crystal layer. A new defect state enters the band gap

To show the continuous modulation of the filter represented in Fig. 3 and 4, Fig. 7 shows the transmission plots corresponding to the quarter-wave reflector with a defect in the middle of again 2370 nm, but for four different states of the liquid crystal:  $\theta = -10, -5, 0$  and  $10$ . In this case the sweep in wavelength is located in the second band gap, and the OSA receives the spectrum filtered. A range of 10 nm can be swept with this design, but it is important to note the non-linearity of the sweep in angle, which depends on the voltage supplied. This effect must be considered so as to control the shift of the wavelength filter, and is located mainly for  $\theta$  between 0 and  $-10$ , as suggested in Ref. 8. Consequently it is guaranteed a tunable filter with linearity response to the voltage applied for a range of 5 nm, corresponding to  $\theta$  between 0 and 10. For a range between  $-10$  and 10 an additional processing of signal is needed.

If the thickness of the defect was reduced the shift in frequency would be lower; that is the sense for selecting a thickness in the limit where more localized modes are created. On the other hand it is also possible to increase the accuracy of the device, if more layers are placed at each side of the defect, because the peaks become thinner. This is shown in Fig. 8 for five different states of the liquid crystal:  $\theta = -3, -3.5, -4, -4.5$  and  $-5$ . The nonlinearity is not appreciated because we are in the range of linearity.

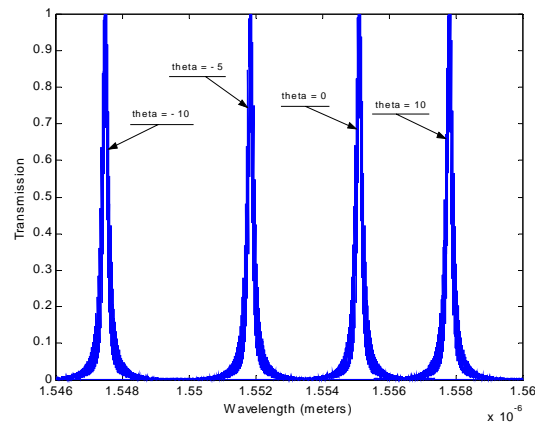


Fig. 7. QWR transmitted power plot for four different states of the liquid crystal

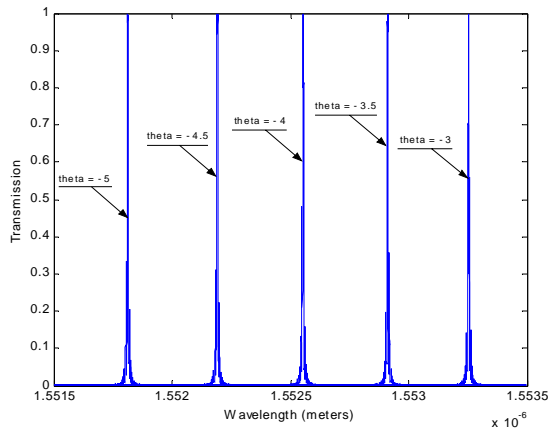


Fig. 8. QWR transmitted power for five refractive indexes in the defect. Number of layers 92

#### 4. Conclusions

In conclusion, it has been analyzed in this work that the localized mode in a 1D-PBG structure with a defect can be exploited in the fabrication of a fiber optic PBG based tunable wavelength filter that detects changes in the voltage applied to smectic A\* liquid crystal

material. By applying an adequate design of the structure, a sweep of 10 nm has been achieved with a region of linearity of 5 nm. The sharpness of the filter can be selected by varying the number of layers at both sides of the liquid crystal layer. The most critical parameter is the thickness of the defect layer, which determines a greater sweep in wavelength if it is increased but at the same time is limited by the appearance of more defect states for higher thicknesses. However, it has been shown that even though this limit is exceeded, there are values where one of the defect states leaves the band gap, which can be exploited for a better sweep in wavelength. Nevertheless, there is also a dependence on the refractive index, which in the example considered does not provoke more defect states, but which must be considered if the refractive index varies more in other designs. This is another application of PBG structures, in this case in one-dimension, and others like the switch of Ref. [8]. An optical refractometer can also be designed by replacing the liquid crystal by the material to be measured, following the rules given.

### **Acknowledgements**

This work was supported by Spanish CICYT TIC 2001-0877-C02-02, Gobierno de Navarra Research Grants, and F.P.U Research Grant supported by Spanish MEC